SUPPLEMENTARY MATERIALS

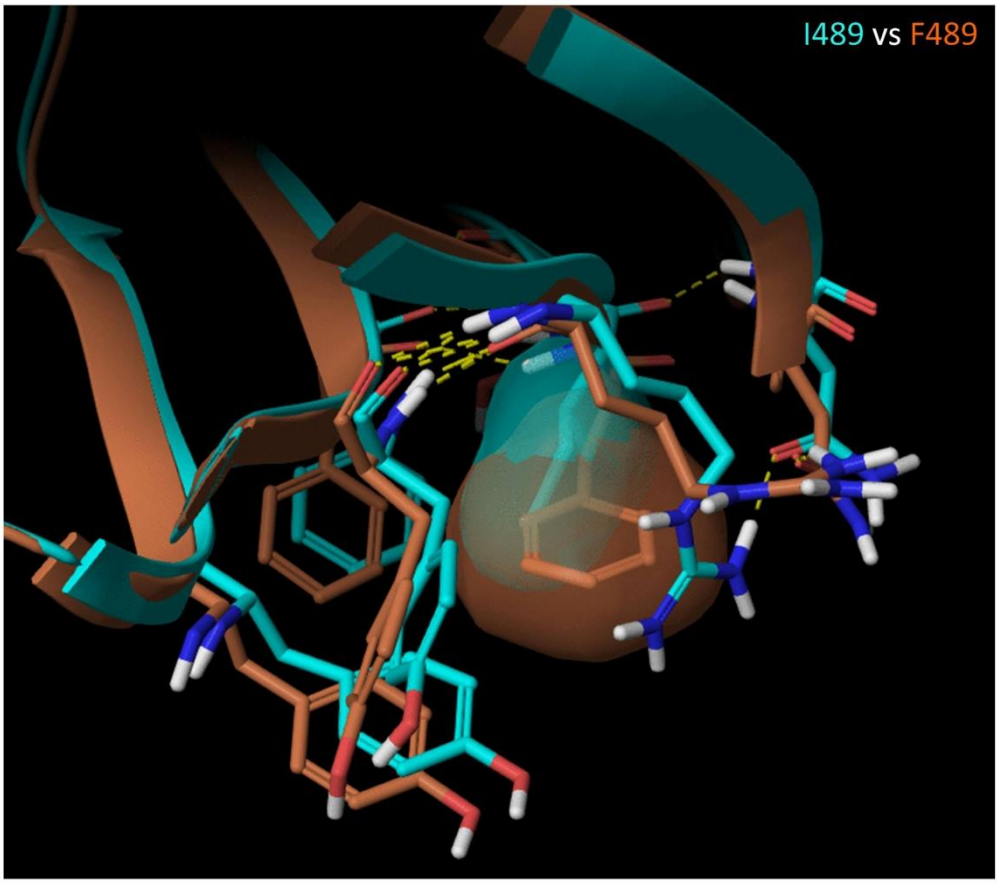

Figure S1. Prediction of Intra C2 domain effect induced by Ile489Phe mutation.

Backbone superimposition of the WT (light blue) and Ile489Phe (rust-coloured) PLCZ1 regions proximal to the mutagenesis site and optimized by molecular dynamics. Briefly, the homology models of the WT and mutant PLCZ1 were generated with the Prime homology modeling workflow (version 3.8, Schrödinger, LLC), using the structure of rPLCδ1 (pdb code: 1DJX) as the template. Upon minimization of the models using Prime's OPLS2005 force field, the models were further optimized via 1.2-ns molecular dynamics simulations (NPT ensemble, 300K, 1 atm, SPC solvent model, 150 mM NaCl) within Desmond (version4.0, D. E. Shaw Research & Schrödinger, LLC). The side chain of the 489 residues are shown as transparent molecular surfaces of the respective colors. In the mutant PLCZ1, adjacent aromatic residues (Y582, F601, Y603) move to accommodate the larger Phe ring, and R487 no longer can or needs to shield Ile489 from the solvent due to lower hydrophobicity of the aromatic Phe. Taken together, these changes are predicted to result in the formation of an aromatic-rich binding sub-site, capable of associating with lipophilic molecules.

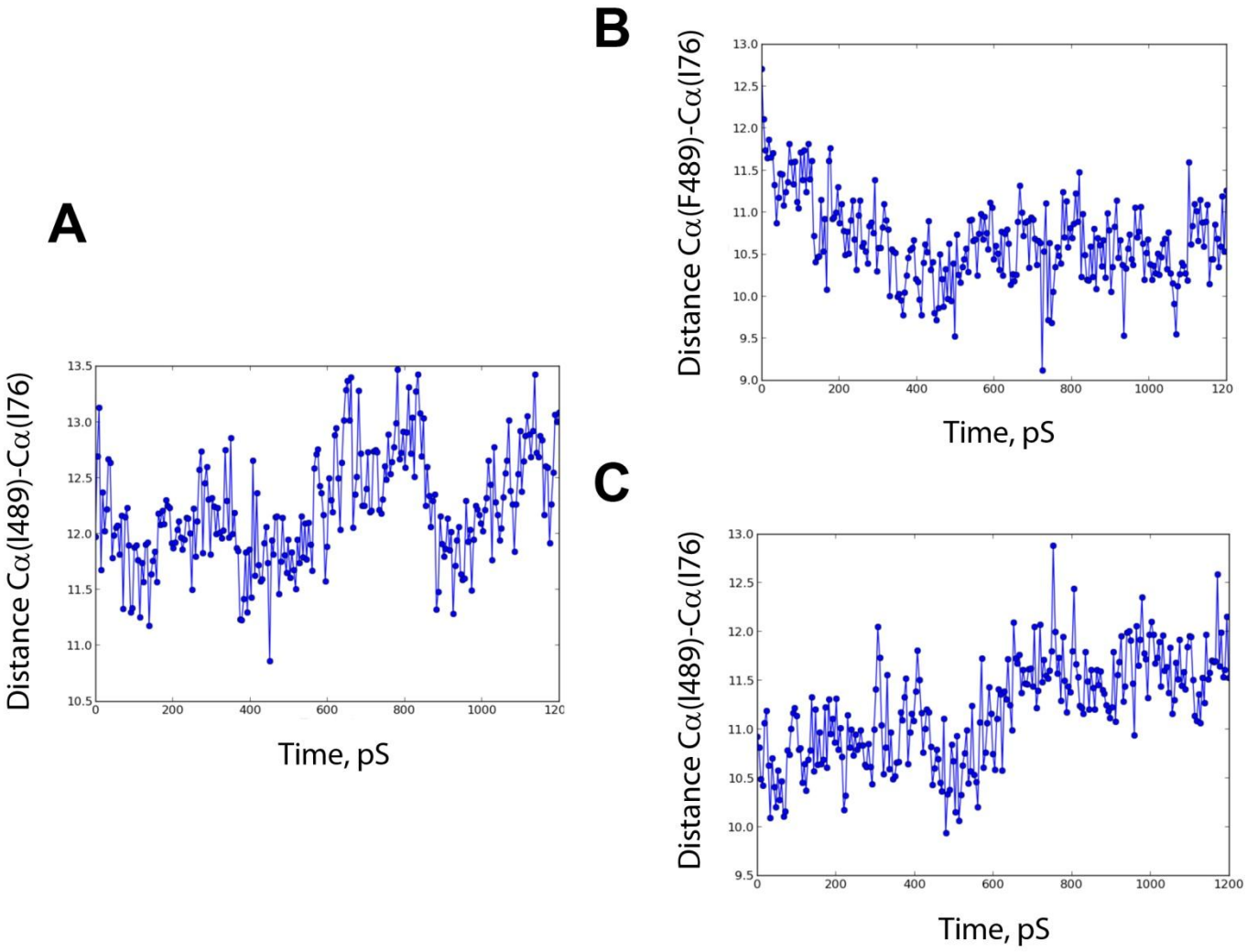

Figure S2. Molecular dynamics simulations of the WT and Ile489Phe PLCZ1 detect a shift of the EF2 hand helix proximal to the mutation site. Topological changes were detected using Simulated Event Analysis program by monitoring the $C\alpha_{I76}$–$C\alpha_{I489}$ and $C\alpha_{I76}$–$C\alpha_{F489}$ distances and root mean square fluctuations (RMSF) as a function of simulation time. The mutant structure from the final frame was modified back to contain Ile489, and a simulation under the identical conditions was conducted to ascertain the persistence of the mutant's conformation. (*A*) The distance between the Cα-Ile76 and Cα-Ile489 atoms of the WT PLCZ1 model is in the 11.0–13.5 Å range (mean: 12.2 Å). (*B*) The distance between the Cα-Ile76 and Cα-Phe489 atoms in the mutant model is reduced to the 9.5–11.5 Å range in the second half of the simulation (mean: 10.7 Å). (*C*) Finally, a WT model, with Ile489 incorporated into the final frame structure of the mutant simulation, returns back to the 11.0–13.0 Å range (Cα-Ile76–Cα-Ile489) by the second half of the simulation.

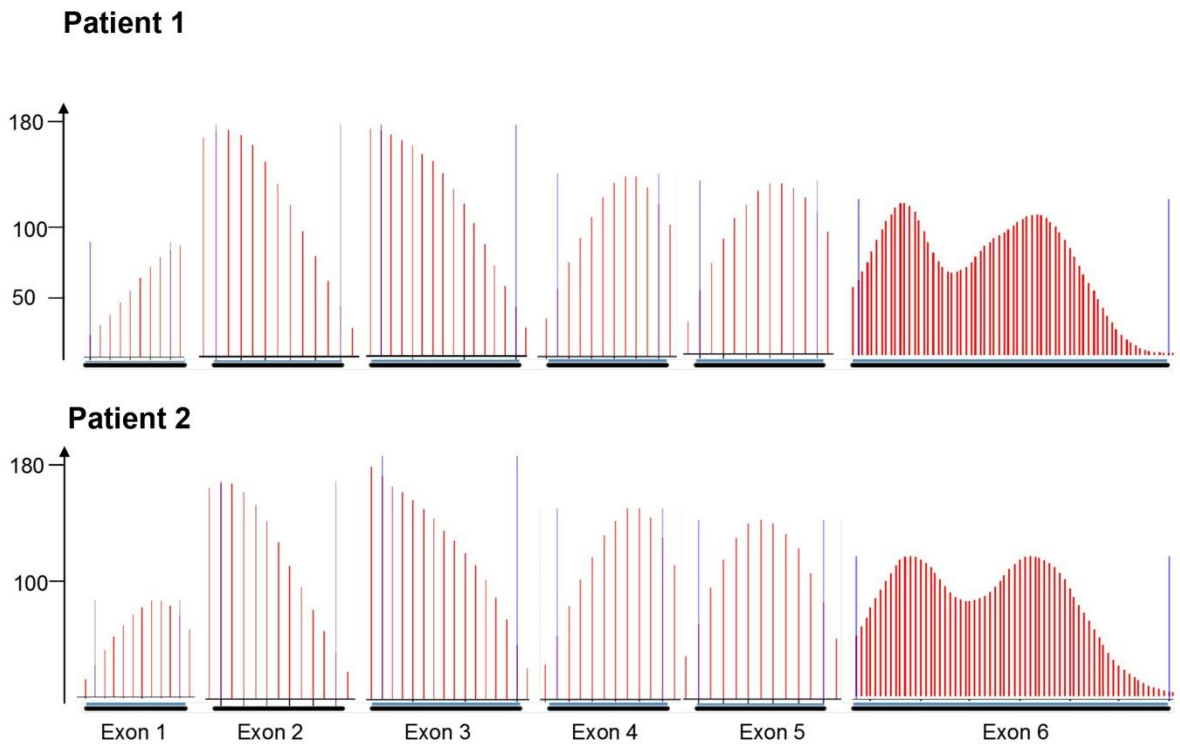

Figure S3. NGS coverage of *WBP2NL* exonic sequence for patients 1 and 2.

The read depth for each patient is indicated in ordinate. For each patient, the minimal coverage for the whole coding sequence is 40X. Note that regions of lesser coverage (beginning of exon 1 and end of exon 6) are the 5' and 3' untranslated regions, respectively.

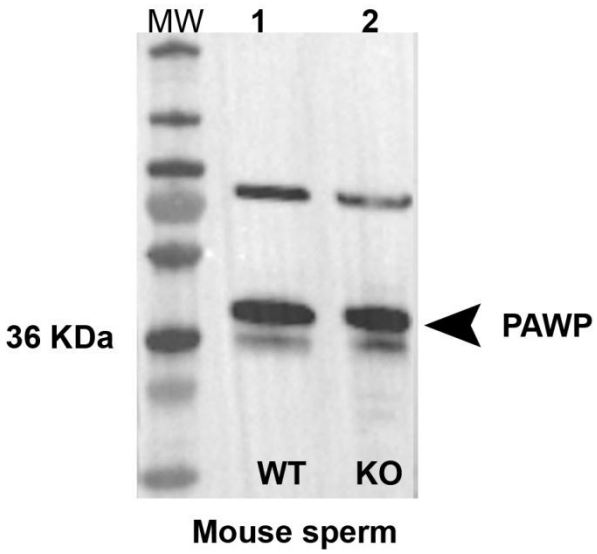

Figure S4. Sperm from *Dpy19l2* KO males show normal expression of PAWP.

WB of protein extracts from sperm of WT (lane 1) and Dpy19l2 KO mice (lane 2) using an anti-PAWP antibody. Immmunoreactivity is observed in the form of a strong band just above 36 kDa, which is near the 37.4 kDa, the expected MW of mouse PAWP, in both lanes.